

# Planet seeding and lithopanspermia through gas-assisted capture of interstellar objects

Evgeni Grishin,<sup>1\*</sup> Hagai B. Perets,<sup>1</sup> Yael Avni<sup>1</sup>

<sup>1</sup>Technion, Israel Institute of technology, Haifa, Israel, 3200003

\*To whom correspondence should be addressed; E-mail: eugeneg@campus.technion.ac.il

**Planet formation begins with collisional-growth of small planetesimals accumulating into larger-ones. Such growth occurs while planetesimals are embedded in a gaseous protoplanetary-disk. However, small-planetesimals experience collisions and gas-drag that lead to their destruction on short-timescales, not allowing, or requiring fine-tuned conditions for the efficient growth of meter-size planetesimals. Here we show that small (up-to 0.1 – 10 km-size) unbound interstellar-objects passing through a gaseous protoplanetary-disk can be efficiently captured to become embedded in the disk. 'Seeding' of such planetesimals then catalyze further planetary-growth into planetary embryos, and potentially alleviate the main-challenges with the meter-size growth-"barrier". Moreover, planetesimal-capture provides a far-more efficient route for lithopanspermia than previously thought, and  $\sim 10^4$  interstellar objects such as the recently detected 1I/2017-U1 ('Oumuamua) could have been captured, and become part of the young Solar System.**

The recent flyby of the interstellar-object 'Oumuamua (*I*) suggests that encounters of interstellar-planetesimals with different solar systems are much more common than previously thought (2).

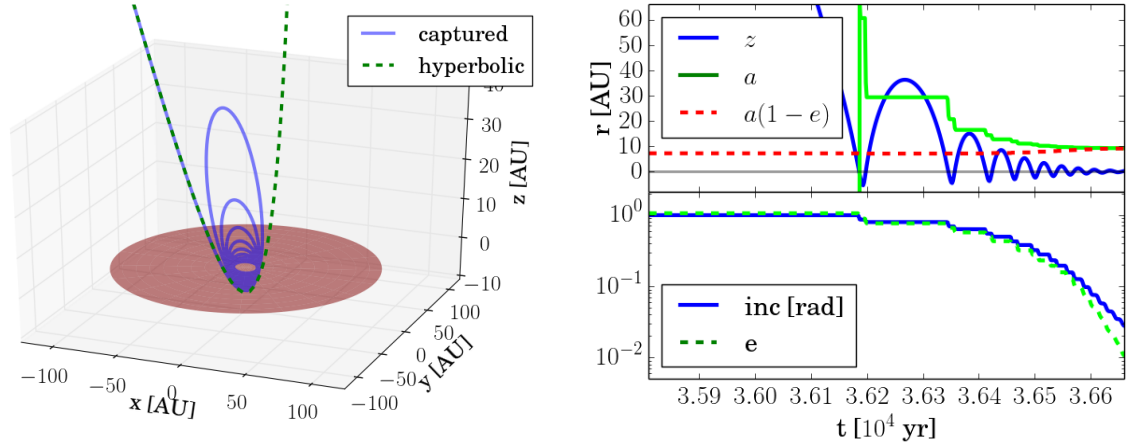


Figure 1: Flyby and capture orbits of interstellar-planetesimals. (a) The 3D trajectories of initially hyperbolic, interstellar-planetesimals. The dashed (green) line represents a hyperbolic (non-capture) encounter, similar case of 'Oumuamua, for planetesimals of size  $R_p = 10^4$  m. The blue line corresponds to a smaller planetesimals ( $R_p = 10$  m) which efficiently dissipates its velocity through gas-drag, decelerates and becomes embedded in the disc (red circle). The initial orbital elements are the same. (b) Time evolution of the orbital elements of the captured orbit. Top panel shows the evolution of the height  $z$  above the protoplanetary-disk, the semi-major axis  $a$  and the pericentre approach  $a(1-e)$ . The bottom panel shows the evolution of the inclination and the eccentricity  $e$ .

Some of these interstellar planetesimals could potentially be recaptured later-on by other stars through dynamical processes (3). This exchange of material is considered as a possible mechanism for lithopanspermia (4–6). However, previously suggested dynamical exchange mechanisms are inefficient; most effective mechanisms require planetesimal encounters with a binary system, and its subsequent capture mostly through collisions with planets (3). Capture of planetary material following the dispersal of the host-cluster is another suggested much more efficient mechanism (7–10). However, it introduces capture at typically large (hundreds to thousands astronomical units; AU) distances from the host star, and it occurs on timescales comparable with the lifetime of the dispersing clusters (up to a few tens of Myrs; larger than the lifetimes of protoplanetary-discs and planet-formation timescales).

Here we show that capture of interstellar-planetesimals can be catalyzed by aerodynamic

gas-drag dissipation during protoplanetary-disc crossing. The gas-drag experienced by small-size planetesimals during their crossing of the disk allows them dissipate their velocity and become bound to the system. Gas-drag induced migration and capture of planetesimals are known to play an important role in planet-formation and the evolution of bound-planetesimals embedded in protoplanetary-disks (11–18). As we show, their role in the evolution of *interstellar*-planetesimals capture is no-less important. Fig. 1 shows examples of typical trajectories and evolution of interstellar-planetesimals as they encounter the disc, dissipate their orbit and become embedded in the disc. In the following we use a detailed analysis to provide a quantitative study of the capture rate of such planetesimals.

Let us consider an interstellar object going through a gaseous protoplanetary disc. For a spherical body with density  $\rho_p = 1 \text{ g cm}^{-3}$ , radius  $R_p$  and relative velocity  $\mathbf{v}_{\text{rel}}$  which crosses a region of the disc with density  $\rho_g$ , the aerodynamic gas drag force is

$$\mathbf{F}_D = -\frac{1}{2}C_D\pi R_p^2\rho_g v_{\text{rel}}^2 \hat{\mathbf{v}}_{\text{rel}}, \quad (1)$$

where  $C_D(\mathcal{R}e)$  is the drag coefficient, which depends on the Reynolds number  $\mathcal{R}e$  (see methods). The body is captured if the loss of energy during the passage  $\Delta E \sim F_D v_{\text{rel}} t_{\text{cross}} \sim C_D R_p^2 \Sigma_g v_{\text{rel}}^2$  is greater than the (positive) kinetic energy at infinity  $E_{\text{inf}} \sim m_p v_{\infty}^2$ . Here  $t_{\text{cross}} \sim h/v_{\text{rel}}$  is the crossing time,  $h$  is the scale-height of the disc,  $v_{\text{rel}}$  is the relative velocity during the passage,  $\Sigma_g$  is the surface density of the disc, and  $v_{\infty}$  is the velocity at infinity of the hyperbolic trajectory. The capture condition for planetesimal sizes is then

$$R_p \lesssim \frac{3}{4} \frac{C_D \Sigma_g}{\rho_p} (1 + \Theta_s), \quad (2)$$

where  $\Theta_s \equiv v_{\text{esc}}^2/v_{\infty}^2$  is the gravitational focusing Safronov number and  $v_{\text{esc}}^2 = 2GM/a \approx v_{\text{rel}}^2 - v_{\infty}^2$  is the escape velocity at closest approach  $a$ . The 3/4 factor comes from more exact derivation (see methods). For  $\Theta_s \gg 1$  gravitational-focusing is important, while for  $\Theta_s \ll 1$

the scattering is mostly in the geometric collision regime.

Taking typical values for the protoplanetary-disc properties (following similar assumptions as in refs. (16, 19) we model different drag laws prescription, and consider a protoplanetary-disc with a radial surface density profile  $\Sigma_g \propto a^{-1}$ . The disc scaling is adapted from the Chiang-Goldreich simple flared disc model (20).

In order to evaluate the fractions and total numbers of planetesimals captured through this process, we need to consider all the relevant encounter properties/parameters and their distributions. These include the velocity distribution; the distribution of impact parameters; the relative impact angles to the disc; and the actual sizes (size-distribution) of the incoming planetesimals. Interstellar-objects likely follow a Maxwellian distribution of the velocity (similar to their progenitor stellar hosts)  $V_\infty \sim \text{Maxwell}(\sigma)$ , where  $\sigma$  is the velocity dispersion. The distribution of impact parameters should follow a simple geometric cross-section, i.e. a uniform distribution of the impact parameter  $B^2 \sim U[0, b_{\text{max}}^2]$  (the trajectory can later change due to gravitational focusing; which we account for when relevant), where  $b_{\text{max}}$  is the maximal impact parameter for an effective close encounter. Both of these depend on the stellar environment.

One may consider two types of environments; (1) A cluster/stellar-association environment in which a group of stars is bound together and their relative velocities are low; and (2) a field environment where stars/interstellar-planetesimals are unrelated to each other and the relative velocities between them is high. Following (3) we use  $\sigma = 6.2 \text{ km s}^{-1}$  and  $b_{\text{max}} = 234 \text{ AU}$  for a cluster environment; and  $\sigma = 40 \text{ km s}^{-1}$  and  $b_{\text{max}} = 130 \text{ AU}$  for the field. Using these we can derive the detailed capture probability for any given environment (see Methods). For the geometric regime ( $\Theta_s \ll 1$ ; corresponding to large impact parameters and/or high velocities), the capture probability is

$$f_c(R_p) \approx \left( \frac{3C_D \Sigma_{g,0}}{4\rho_p R_p} \right)^2 \left( \frac{b_{\text{max}}}{\text{AU}} \right)^{-2} = 0.6 \left( \frac{C_D}{24} \right)^2 \left( \frac{b_{\text{max}}}{234 \text{ AU}} \right)^{-2} \left( \frac{R_p}{2 \text{ m}} \right)^{-2}, \quad (3)$$

where the latter underestimates the effect of gravitational focusing for rocks of size  $\gtrsim 10$  m in clusters and  $\gtrsim 10^2$  m in the field. In the gravitational focusing regime, ( $\Theta_s \gg 1$ ; which corresponds to small impact parameters and/or low velocities), the capture probability is

$$f_c(R_p) \approx \frac{x^{3/2}}{\sqrt{2\pi}} (\ln(1/x) + 0.78), \quad (4)$$

where

$$x = \left( \frac{6C_D \Sigma_0}{\rho_p R_p} \right)^{1/3} \frac{GM}{\sigma^2 b_{\max}} \left( \frac{b_{\max}}{\text{AU}} \right)^{-1/3}, \quad (5)$$

where the choice of the drag coefficient for each regime is described in the methods section.

For large planetesimals, the power law dependence is

$$f_c(R_p) \approx 10^{-3} \left( \frac{C_D}{0.44} \right)^{1/2} \left( \frac{\sigma}{6.2 \text{ km/s}} \right)^{-3} \left( \frac{b_{\max}}{234 \text{ AU}} \right)^{-2} \left( \frac{R_p}{10^3 \text{ m}} \right)^{-1/2}, \quad (6)$$

In order to better verify the analytic probabilistic estimates, we run N-body simulations that include gravity and a prescription for gas drag (Eqn. 1), based on 4th order Hermite integrator (21). For each planetesimal-size we run  $10^4 - 2 \cdot 10^5$  numerical integrations with  $b$  and  $v_\infty$  distributed as described above. The relative angles between the planetesimal trajectories and the protoplanetary-disc were drawn from an isotropic distribution (uniform in the argument of pericentre and the longitude of ascending node angles, and uniform in the cosine of the inclination angle). Figure 1 shows two examples of capture trajectories. Fig. 2 shows the comparison between the analytic estimates and the simulations. Small planetesimals, up to  $\sim 10$  m, are the most susceptible to gas drag, and are efficiently captured. These can be captured even at the lower density regimes of the disc at large separations; hence, their capture fractions are far higher than larger planetesimals. The latter are typically captured only when the pericentre approach of their trajectory is sufficiently close to the high-density inner regions of the disc. We can now estimate the total number of captured objects by convoluting the capture probability with the expected size distribution of interstellar-planetesimals (see methods).

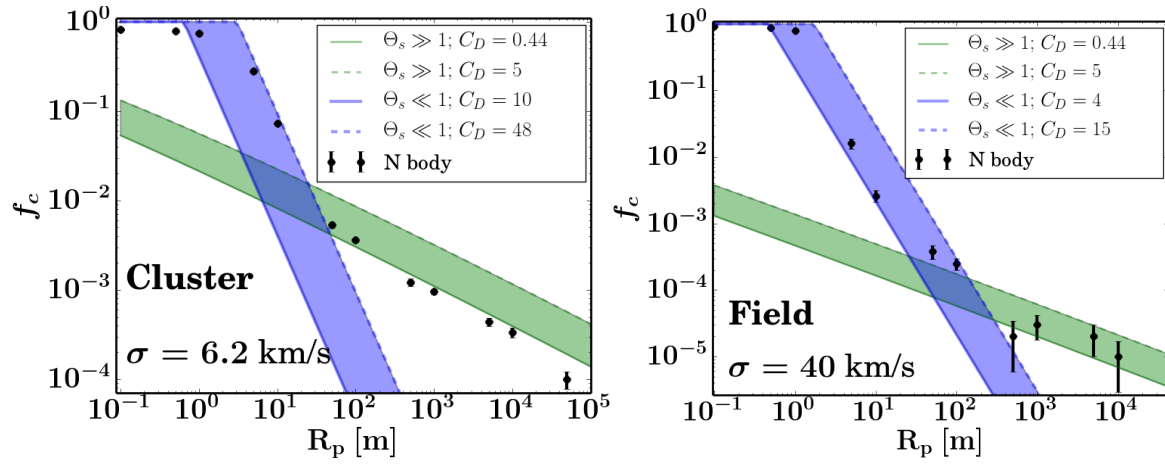


Figure 2: Fractions of captured planetesimals as a function of their size. Blue area is the estimated probability in the geometric scattering regime, green area is the estimated probability in the gravitational focusing regime. Black dots are result of a numerical simulation. The error bars are estimated from shot noise of the captured orbits. Choices of drag coefficients are discussed in the methods. Generally, planetesimals above  $R_p \gtrsim 100$  m follow the gravitational focusing prediction  $f_c \propto R_p^{-1/2}$ . The transition to geometric scattering regime is near  $\sim 10$  m for cluster environment and  $\sim 100$  m for field environment and is understood from the difference in the velocity dispersion of each environment.

Using the size-dependent capture-probability, we obtain the total number of captured planetesimals of a given size. During the planet formation process, a large amount of planetesimals is ejected from a given planet-forming system, and these become unbound interstellar-objects (22, 23). These ejections occur both during the early planet formation phase, or on longer timescales throughout the stellar and dynamical evolution of the system, long after the protoplanetary-disc dissipates. Adams et al. (3) estimate that for each young star at least  $\gtrsim M_{\oplus}$  of solids are ejected into the interstellar medium (ISM) with a typical ejection velocity of  $\langle v_{\text{eject}} \rangle = 6.2 \pm 2.7 \text{ km/s}$ . They consider a mass function of  $dN/dm \propto m^{-p}$ , which is also consistent with recent aerodynamically coupled gas-particle mixture simulations yielding  $p = 1.6 \pm 0.1$  (24) (though the mass-function could be more top-heavy when accounting for tidal disruption of planetesimals near a giant planet (25)). We use similar assumptions, and consider the same velocities, and take  $p = 5/3$  in order to estimate the total numbers of ejected interstellar-planetesimals,  $N_{\text{eject}}$ .

The number of ejected planetesimals of mass  $> m_1$  is then  $N_{\text{eject}}(m > m_1) \sim (m_1/M_{\oplus})^{-2/3}$ . The number of planetesimals entering the disc region is therefore  $N_{\text{enter}} \approx n_{\text{ISM}} \sigma_E \langle v \rangle \tau$ , where  $n_{\text{ISM}} = n_{\star} N_{\text{eject}}$  is the number density of interstellar-planetesimals,  $n_{\star}$  is the number density of stars,  $\sigma_E = \pi b_{\text{max}}^2$  is the cross section, with a maximal impact parameter  $b_{\text{max}}$ , above which no significant encounter occurs, and  $\langle v \rangle$  is the relative velocity.  $\tau$  is a typical timescale during which encounters with the disk can occur, as we discuss below. For the cluster environment we consider a stellar density of  $n_{\star}^c \sim 750/\pi N_{\star}^{1/2} \text{ pc}^{-3}$ , where  $N_{\star} = 100 - 1000$ . In this case, the velocity is dominated by the dispersion velocity of ejected planetesimals  $\langle v_{\text{eject}} \rangle = 6.2 \pm 2.7 \text{ km/s}$ . Encounters in a young cluster environment can occur only during the time where the ejected planetesimals still reside in the cluster. The faster planetesimals are unbound to the cluster and reside in it only during their first crossing time of the cluster  $\tau_{\text{cl}} \sim r_{\text{cl}}/\langle v \rangle \sim 0.3 \text{ Myr}$ . However, a fraction of the interstellar-planetesimals (6% for the Maxwellian distribution) have low

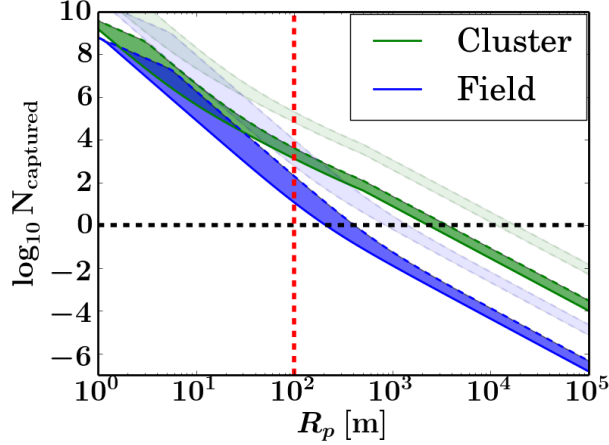


Figure 3: The number of captured planetesimals during disc lifetime of  $t_{disc} = 3 \text{ Myr}$ , given the theoretically estimated rates. Green areas are the confined rates for clusters, while blue areas are the confined rates for fields. The boundaries are determined by different drag coefficients, similar to Fig. 2. Red vertical line stands for the effective radius of 'Oumuamua,  $\sim 100 \text{ m}$ . The observed rate, based on 'Oumuamua passage, are enhanced by  $\sim 50$  times. The enhanced rates represented by the transparent green and blue areas for the cluster and the field, respectively.

velocities  $\lesssim 1 \text{ km/s}$  and are bound to the cluster. These can encounter protoplanetary-disks throughout the disk-lifetime, i.e. for these  $\tau \approx t_{disc} = 3 \text{ Myr}$ . These are also more likely to be captured during their crossing of a protoplanetary-disk ( $\sim 25\%$  of the captured large planetesimals have velocities lower than  $1 \text{ km/s}$ ). Thus, the total number of entering planetesimals is  $N_{\text{enter}}^c = n_{\text{ISM}} \sigma_E t_{disc} (\tau_{cl}/t_{disc} + f_b (1 - \tau_{cl}/t_{disc}))$ , where  $f_b = 0.06$ .

In the field, the velocity is dominated by the (observed) stellar velocity dispersion  $\langle v \rangle = \sigma \approx 40 \text{ km/s}$ , the stellar density is  $n_*^f \sim 0.1 \text{ pc}^{-3}$  and  $\tau = t_{disc} = 3 \text{ Myr}$ . Plugging in the numbers, the number of planetesimals entering a protoplanetary-disk during its lifetime is  $N_{\text{enter}}^c(R > 1 \text{ km}) \approx 7 \cdot 10^3 (R/1 \text{ km})^{-2}$  in a cluster environment, and  $N_{\text{enter}}^f(R > 1 \text{ km}) \approx 620 (R/1 \text{ km})^{-2}$  in the field. This is likely a lower-limit, since the inferred encounter rate of 'Oumuamua-like objects (with effective diameter of  $\sim 100 \text{ m}$ ), given its recent detection, is  $\sim 50$  times higher than the above-estimated rate for  $100 \text{ m}$ -size bodies entering the Solar system in today's field environment (2).

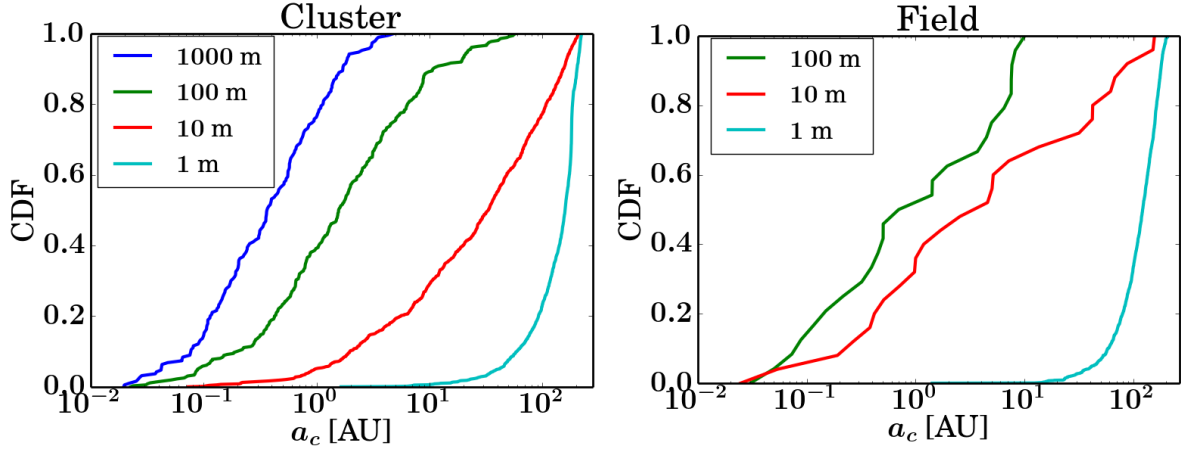


Figure 4: The size dependent cumulative radial distribution of captured planetesimals. Several planetesimal sizes are shown;  $R_p = 5000, 100, 10, 1$  m (blue, green, red and cyan, respectively), for the cluster (left) and the field (right). Once captured, the circularization timescale is much shorter than radial drift timescales (see Fig. 1b and (11)), thus the final semi-major axis is close to the first pericentre approach.

Figure 3 shows the expected size-dependent number of captured planetesimals. At least one planetesimals as large as  $\sim 2$  km ( $\sim 0.2$  km) is captured in a cluster (field) environment. The inferred rate, based on 'Oumuamua passage, is enhanced by  $\sim 50$  times. The latter would then results the capture of even  $\sim 11$  km ( $\sim 0.8$  km) for a cluster (field) environment. Note that in either estimate of the capture fraction (Eq. 3 and 4) it is proportional to  $\propto b_{\max}^{-2}$ , which cancels out with the  $\propto b_{\max}^2$  from the encounter rate. Thus, the total number of captured planetesimals  $N_{\text{enter}} \cdot f_c$  is independent of  $b_{\max}$ , hence the choice of  $b_{\max}$  is rather arbitrary, as expected.

Fig. 4 shows the empirical cumulative radial distribution of captured planetesimals for different size ranges. As mentioned above, disc dissipation can be efficient for small planetesimals even at the disc outskirts where the gas densities are low. The capture of larger planetesimals, however, requires higher gas-densities. Therefore the larger the planetesimals, the more centrally concentrated is their radial distribution.

The disc-capture scenario presented here allows for efficient capture of hundreds of large

planetesimals, and numerous smaller planetesimals and large dust grains. These large dust-grains and/or large planetesimals can then serve as seeds for planetary growth that can catalyze planet formation (26, 27), and overcome the meter-size barrier. During their growth the now-even-larger planetesimals collide, some of them fragmenting and re-populating the intermediate km-size population with new planetesimals. A fraction of these are later ejected from the systems, and further replenish the population of interstellar-planetesimals. These, in turn, can be recaptured by other systems and further catalyze planet-formation, and so on, i.e. leading to a chain-reaction – like exponential planets seeding process.

One may still question how did large planetesimals and later planets formed in the first system that initialized the seeding. Formation of km-sized planetesimals is a long-standing problem in planet-formation theories (see refs. (14, 28) for reviews, suggested solutions and their difficulties). The disc-capture can not account for this initial formation, however, it can alleviate the problem, by allowing for the first formation of such planetesimals to be a rare event, and even under fine-tuned condition. Most stars are thought to form in stellar associations and clusters. If only a few large (0.5 – 1 km) planetesimals are sufficient for seeding a given planetary-system (e.g. ref. (26, 29)), or a larger number of smaller planetesimals (30)), then given the above-calculated rates  $N_{\text{enter}}(> 0.5 \text{ km}) \cdot f_c(> 0.5 \text{ km}) \sim 2.8 \cdot 10^4 \cdot 2 \cdot 10^{-3} (R_p/0.5 \text{ km})^2 \sim 60$  large planetesimals are captured by a given system (and numerous smaller ones). In other words, 1 – 2% (or less, in the case where smaller planetesimals are required (30)) of the systems are needed to form in-situ large planetesimals and produce interstellar-planetesimals. In other words, a small fraction of planetary systems is needed in order to seed all of the other protoplanetary-systems in the cluster. If the  $\sim 50$  times higher rates directly inferred from 'Oumuamua detection are taken at face value, a much smaller number is required, and even a field environment could be sufficient, i.e. even the first planet-forming system in the cluster could have been seeded by itself from field interstellar-planetesimals.

Planetesimal ablation could potentially affect, or even destroy a planetesimal as it crosses a protoplanetary-disc for the first-time at high velocity. However, using simplified ablation models (based on ref. (31); see methods) we find that at most  $\sim 12\%$  of icy-planetesimals and  $\sim 5\%$  of rocky-planetesimals of  $10 - 10^3$  m sizes are ablated during crossings in stellar clusters, and  $\sim 30\%$  icy and  $\sim 15\%$  rocky planetesimals of  $10 - 10^2$  m are ablated in field environments. These do not significantly affect the overall results.

The composition of meteorites in the Solar System is typically thought to relate to the primordial composition of the protoplanetary-disc. However, there is evidence for the existence of material captured from external sources. In particular, there is evidence for short-lived radioactive nuclei which were likely formed in a relatively nearby supernovae (32). In addition, analysis of heavy  $^{60}\text{Fe} - ^{60}\text{Ni}$  isotopes in asteroids suggests the early injection of  $^{60}\text{Fe}$  into the primordial protoplanetary-disc of our Sun (33). The disc-capture mechanism allows for embedding such external material in the disc, and may help explain its origin. These issues are not the main focus of our study, but it is interesting to consider the possibility of composition peculiarities in some meteorites originating from capture of material from other systems through this process.

Finally, rocks more massive than 10 kg could shield biologically active material from extreme radiation (23) and pressure (34). The disc capture scenario predicts  $\sim 10^9$  captures of 10 kg planetesimals by a protoplanetary-disc in the field and  $\sim 10^{12}$  captures in cluster environments. If we assume, following (3), that  $10^{-13}$  (only  $10^{-9}$  of the planetesimals are assumed to contain biologically active material, and only  $10^{-4}$  impact the surface of terrestrial planets) of such biologically-active planetesimals give rise to a lithopanspermia event, then one in ten systems could have experienced a lithopanspermia event, even before accounting for the possibly higher rate inferred by 'Oumuamua. This makes the possibility that the Earth itself may have had such an event non-negligible (and  $\sim 10^2 - 10^5$  times more likely than suggested in

previous studies (3)).

## Methods

In the following we provide a detailed derivation of the analytic calculations of the capture probability discussed in the main text. As mentioned above, these results support and agree with the full N-body simulation results.

### Exact derivation of the capture condition

For a planetesimal that crosses the disc face on at radial location  $a_{\text{cross}}$ , the amount of energy loss during the interaction with the disc is the total work applied on the planetesimal

$$\Delta E = \int \mathbf{v}_{\text{rel}} \cdot \mathbf{F}_p dt \approx -\frac{1}{2} C_D \pi R_p^2 \rho_g(a_{\text{cross}}) \int_{-\infty}^{\infty} \exp\left(-\frac{v_{\text{rel}}^2 t^2}{2h^2}\right) v_{\text{rel}}^3 dt \quad (7)$$

$$= -\frac{1}{2} C_D \pi R_p^2 \Sigma_g v_{\text{rel}}^2 \quad (8)$$

where  $\mathbf{v}_{\text{rel}} = \mathbf{v}_{\infty} + \mathbf{v}_{\text{esc}}(a_{\text{cross}})$ . Since we deal with regimes where either  $v_{\infty} \gg v_{\text{esc}}$  or  $v_{\infty} \ll v_{\text{esc}}$ ,  $v_{\text{rel}}^2 \approx v_{\infty}^2 + v_{\text{esc}}^2$  takes both options into account. The initial energy is  $E_{\text{in}} = 0.5 m_p v_{\infty}^2$ , and the fractional energy loss  $|\Delta E|/E_{\text{in}}$  gives Eq. (2).

### Capture fractions

The distributions for the velocity and impact parameter are

$$f_V(v, \sigma) = \sqrt{\frac{2}{\pi}} \frac{v^2}{\sigma^3} \exp\left(-\frac{v^2}{2\sigma^2}\right); v \in [0, \infty] \quad (9)$$

$$f_B(b, b_{\text{max}}) = \frac{2b}{b_{\text{max}}^2}; b \in [0, b_{\text{max}}] \quad (10)$$

where  $f_V(v, \sigma)$  is Maxwellian distribution with velocity dispersion  $\sigma$ ,  $b_{\text{max}}$  is the maximal impact parameter considered. In what follows, we will separate the capture condition (Eq. 2)

into terms that depend on the disc and the planetesimal parameters  $(C_D, \Sigma_g, \rho_p, R_p)$  and on the initial encounter parameters  $(b, v_\infty)$  only. Then we determine the capture probability for each regime.

## Geometric scattering

In this case  $\Theta_s \ll 1$  (negligible gravitational focusing), i.e. the trajectory of an incoming interstellar-planetesimals follows a straight line before encountering the disc, and is negligibly affected by the gravitational pull from the host star. The capture criteria is then

$$\frac{3C_D \Sigma_g}{4\rho_p R_p} < 1 \quad (11)$$

taking a density profile  $\Sigma_g = \Sigma_{g,0}(a/\text{AU})^{-\beta}$  we get

$$\left(\frac{a}{\text{AU}}\right)^\beta < \frac{3C_D \Sigma_{g,0}}{4\rho_p R_p} \quad (12)$$

For geometric scattering, the closest approach is  $q \approx b$ , so the criteria is

$$b < \left(\frac{3C_D \Sigma_{g,0}}{4\rho_p R_p}\right)^{1/\beta} \text{AU} \quad (13)$$

or with the dimensionless parameter  $x = b/b_{\text{max}}$ , the capture probability is

$$P(x < x_{\text{max}}) = x_{\text{max}}^2 = \left(\frac{3C_D \Sigma_{g,0}}{4\rho_p R_p}\right)^{2/\beta} \left(\frac{\text{AU}}{b_{\text{max}}}\right)^{-2} \quad (14)$$

Since  $x \propto R_p^{-2}$ , in the ram pressure regime we predict the capture fraction  $f_c \propto R_p^{-2}$ . As we shall see, it underestimates the capture fraction for large planetesimals.

## Gravitational focusing

In this case  $\Theta_s \gg 1$ , and the effective closest approach could be significantly smaller than the initial impact parameter at infinity, due to the gravitational pull of the host star. The capture condition (Eq. 2) is

$$\left(\frac{a}{\text{AU}}\right)^\beta v_\infty^2 < \frac{3C_D \Sigma_{g,0}}{2\rho_p R_p} \frac{GM}{a} \quad (15)$$

In order to proceed, we use the parabolic approximation to find the closest approach  $a \approx q$  :

$$q = \frac{GM}{v_\infty^2} \left[ \sqrt{1 + \frac{b^2 v_\infty^4}{G^2 M^2}} - 1 \right] \approx \frac{b^2 v_\infty^2}{2GM} \quad (16)$$

so the capture condition is

$$b^{(2+2\beta)/(2+\beta)} v_\infty^2 = \left( \frac{3 \cdot 2^\beta C_D \Sigma_{g,0}}{\rho_p R_p} \right)^{1/(2+\beta)} GM \cdot \text{AU}^{\beta/(2+\beta)} \quad (17)$$

Now we define a new random variable  $x \equiv (b/b_{\max})^\alpha (v_\infty/\sigma)^2$ , and find its distribution function  $f_X(x)$ .

First, we transform to  $k = b^\alpha$  and  $dk = \alpha b^{\alpha-1} db$ , so

$$f_K(k) = f_B(b) \frac{db}{dk} = \frac{2b^{(2-\alpha)/\alpha}}{\alpha b_{\max}^2} \quad (18)$$

similarly, the distribution function of  $u \equiv v^2$  is

$$f_U(u) = \sqrt{\frac{2}{\pi}} \frac{u^{1/2}}{\sigma^3} e^{-u/2\sigma^2} \quad (19)$$

Now, the distribution of  $z \equiv b^\alpha v^2$  is given by

$$f_Z(z) = \iint f_U(t) f_K(k) \delta(ku - z) dk du \quad (20)$$

$$= \iint \sqrt{\frac{8}{\pi}} \frac{u^{-1/2} e^{-u/2\sigma^2} k^{(2-\alpha)/\alpha}}{\alpha \sigma^3 b_{\max}^2} \delta\left(k - \frac{z}{u}\right) dk du \quad (21)$$

$$= \sqrt{\frac{8}{\pi}} \frac{z^{(2-\alpha)/\alpha}}{\alpha \sigma^3 b_{\max}^2} \int_{z/k_{\max}}^{\infty} u^{(\alpha-4)/2\alpha} e^{-u/2\sigma^2} du \quad (22)$$

where  $\delta(y)$  is the Dirac delta function and  $k_{\max} = b_{\max}^\alpha$ . Finally, setting  $x = z/b_{\max}^\alpha \sigma^2$  we get

$$f_X(x) = \frac{1}{\alpha} \sqrt{\frac{8}{\pi}} x^{(2-\alpha)/\alpha} \int_x^{\infty} w^{(\alpha-4)/2\alpha} e^{-w/2} dw \quad (23)$$

$$= \frac{2^{2-2/\alpha}}{\alpha \sqrt{\pi}} x^{(2-\alpha)/\alpha} \Gamma\left(\frac{3\alpha-4}{2\alpha}, \frac{x}{2}\right) \quad (24)$$

where  $w = u/\sigma^2$  and  $\Gamma(s, y) = \int_y^\infty y^{s-1} e^{-y} dy$  is the upper incomplete gamma function. Getting back to  $\alpha(\beta) = (2 + 2\beta)/(2 + \beta)$  leads to

$$f_X(x) = 2^{\beta/(1+\beta)} \frac{2 + \beta}{(2 + 2\beta)\alpha\sqrt{\pi}} x^{(1/(1+\beta))} \Gamma\left(\frac{\beta - 1}{2\beta + 1}, \frac{x}{2}\right) \quad (25)$$

The cumulative distribution is  $F_X(x) = \int_0^x f_X(x') dx'$ . For a given size  $R_p$ , the capture probability is

$$P = \int_0^{x_{\max}} f_X(x) dx = F_X(x_{\max}) \quad (26)$$

where  $x_{\max}(R_p)$  is the largest parameter allowed by the capture condition given in Eq. 2.

To compare with numerical simulations, we take  $\beta = 1$  and the probability distribution is

$$f_X(x) = \frac{3}{\sqrt{8\pi}} x^{1/2} \Gamma(0, x/2) = -\frac{3}{\sqrt{8\pi}} x^{1/2} \text{Ei}(-x/2) \quad (27)$$

where  $\text{Ei}(y) = -\int_{-y}^\infty (e^{-y'}/y') dy'$  is the exponential integral. The maximal dimensionless parameter is (Eq. 5)

$$x_{\max} = \left(\frac{3C_D \Sigma_{g,0}}{\rho_p R_p}\right)^{1/3} \frac{GM}{b_{\max}^{4/3} \sigma^2} \cdot \text{AU}^{1/3} \quad (28)$$

The probability is

$$P(x < x_{\max}) = \text{erf}\left(\sqrt{\frac{x_{\max}}{2}}\right) - \frac{x_{\max}^{3/2} \text{Ei}\left(-\frac{x_{\max}}{2}\right)}{\sqrt{2\pi}} + \sqrt{\frac{2}{\pi}} x_{\max}^{1/2} e^{-x/2} \quad (29)$$

a decent rational approximation near  $x_{\max} = 0$  is

$$P(x_{\max}) \approx \sqrt{\frac{1}{2\pi}} \left\{ -x_{\max}^{3/2} \ln x_{\max} + x_{\max}^{3/2} (\ln 2 + \frac{2}{3} - \gamma) + \frac{3}{10} x_{\max}^{5/2} + \mathcal{O}(x_{\max}^{7/2}) \right\} \quad (30)$$

where  $\gamma \approx 0.577$  is the Euler-Mascheroni constant. For small values of  $x_{\max}$  the leading term is  $\propto x_{\max}^{3/2} (\ln(1/x_{\max}) + \tilde{\gamma})$ , where  $\tilde{\gamma} \approx \ln 2 + 2/3 - \gamma = 0.78$ , so the probability is  $\propto x_{\max}^{3/2}$  up to a logarithmic correction. The capture probability is

$$P(R_p) = \sqrt{\frac{1}{2\pi}} x_{\max}^{3/2} (\ln(1/x_{\max}) + \tilde{\gamma}) \quad (31)$$

Ignoring the logarithmic correction gives Eq. (6) where we predict that the capture fraction is  $f_c \propto R_p^{-1/2}$ .

## Drag coefficient

The drag coefficient depends on the size of the planetesimal via the Reynolds number  $Re \sim R_p v_{\text{rel}} / \nu_m$ , where  $\nu_m = (1/2) \bar{v}_{th} \lambda$  is the molecular viscosity of the gas,  $v_{th}$  is the thermal velocity and  $\lambda$  is the mean free path of gas-gas collisions. Large planetesimals are in the ram pressure regime with constant coefficient  $C_D = 0.44$ . Small dust grains are in the Epstein regime, with  $C_D \propto R_p^{-1}$ . The transition to Stokes regime occurs at  $R_p = 9\lambda/4$ . In the Stokes regime,  $C_D \propto R_p^{-3/5}$ . We follow (16) for prescription for the Reynolds number and drag laws. For the gravitational focusing model we account mainly for large planetesimals, thus we expect that the drag coefficient is ram pressure dominated ( $C_D = 0.44$ ) in this regime. For geometric scattering we expect to be somewhere near the Epstein-Stokes transition, i.e. near  $C_D = 24$ .

Planetesimals on cluster environments have lower relative velocities in the geometric regime, and are captured at larger separations compared to field environments. These two effects decrease the Reynolds number and consequently enhance the drag coefficient.

## Capture rates

For field environments, the convolution is just a multiplication  $N_{\text{captured}}(R_p) = N_{\text{enter}}(R_p) \cdot f_c(R_p)$ . For cluster environments there are two different populations, the bound ( $v_\infty < 1$  km/s) and unbound ( $v_\infty > 1$  km/s). Though the bound population consists only of 6% of planetesimals, they are  $\sim 25\%$  of the total captured rates for sizes above  $R_p \gtrsim 0.5$  km. Below  $R_p \lesssim 50$  m the fraction of bound captured planetesimals is  $\sim 6\%$ , as expected from geometric capture. We use a piecewise-continuous linear function of the bound captured planetesimals,  $f_{c,b}(R_p)$ . Given the nominal rate,  $N_{\text{nom}}(R_p) = n_{\text{ISM}} \sigma_E \pi b_{\text{max}}^2 t_{\text{disc}} f_c(R_p)$ , the actual rate from

the two population convolution is

$$\frac{N_{\text{actual}}(R_p)}{N_{\text{nom}}(R_p)} = \frac{\tau_{\text{cl}}}{t_{\text{disc}}} + f_{c,b}(R_p) \left(1 - \frac{\tau_{\text{cl}}}{t_{\text{disc}}}\right) = 0.1 + 0.9f_{c,b}(R_p) \quad (32)$$

For small pebbles  $f_{c,b} = 0.06$  and  $N_{\text{actual}}$  is reduced to  $\sim 15\%$  of the nominal value. For large planetesimals,  $f_{c,b} = 0.25$  and  $N_{\text{actual}}$  is reduced to  $\sim 30\%$  of its nominal value.

## Planetesimal ablation

The ablation equation is (31)

$$\frac{dm}{dt} = -\frac{C_H \rho_g v_{\text{rel}}^3 \pi R^2}{2 Q_{\text{abl}}} \quad (33)$$

where  $m = 4\pi R^3 \rho_p / 3$  is the mass,  $\rho_p$  is the solid density,  $\rho_g$  is the gas density,  $C_H$  is the dimensionless heat transfer coefficient,  $v_{\text{rel}}$  is the relative velocity,  $R$  is the radius and  $Q_{\text{abl}}$  is the specific ablation heat per unit mass. The ablation time is

$$t_{\text{abl}} = \left| \frac{R}{dR/dt} \right| \approx \frac{8}{C_H} \frac{\rho_p}{\rho_g} \frac{Q_{\text{abl}}}{v_{\text{rel}}^3} R \approx 10^4 \left( \frac{R}{m} \right) \left( \frac{a}{\text{AU}} \right)^{53/14} \text{ s} \quad (34)$$

Significant ablation occurs if the ablation times is shorter than the minimum of the disc crossing time  $t_{\text{cross}}$  and the stopping time  $t_{\text{stop}} = |mv_{\text{rel}}/F_{\text{D}}|$ . For pebbles of  $\gtrsim 1$  or larger bodies, the crossing time  $t_{\text{cross}} = h/v_{\text{rel}}$  is the relevant. Comparing the timescale gives the condition for ablation. The critical radial disc separation for ablation as a function of the planetesimal size and disc and planetesimal parameters is

$$a_c = \sqrt{\frac{C_H \rho_g h v_{\text{rel}}^2}{8 \rho_p R Q_{\text{abl}}}} \text{ AU} \quad (35)$$

For typical compositions of ices (see Table 1 of ref. (31)),  $C_H = 0.01$ ,  $Q_{\text{abl}} \approx 3 \cdot 10^{10} \text{ erg g}^{-1}$ ,  $\rho_p = 1 \text{ g cm}^{-3}$  and  $\rho_p$  and  $v_{\text{rel}} \approx v_{\text{esc}}$  normalized to their values at 1 AU the critical radial separation is

$$a_c = \left( \frac{R}{7.3m} \right)^{-1/2} \text{ AU} \quad (36)$$

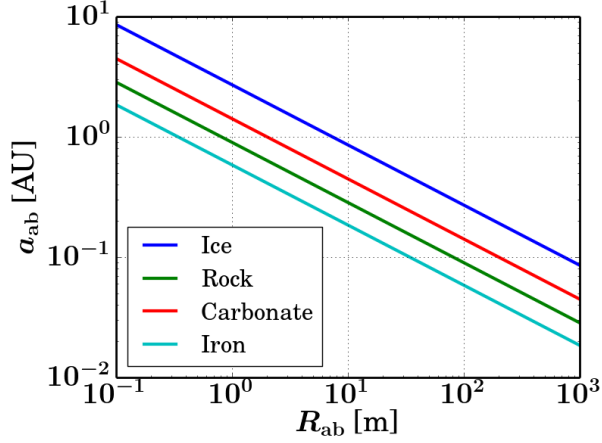


Figure 5: Critical separations for significant planetesimal ablation. Specific ablation heat coefficients and densities are taken from Table 1 of (31)

Cluster	$R_p = 1$ m	$R_p = 10$ m	$R_p = 10^2$ m	$R_p = 10^3$ m
Ice	< 0.1%	4%	12%	12%
Carbonate	< 0.1%	2%	8%	7%
Rock	< 0.1%	1.5%	5%	3%
Iron	< 0.1	< 1%	2%	2.5%

Table 1: Fraction of captured planetesimals lost due to ablation in cluster environments.

Figure 5 shows the critical separation as a function of the planetesimal size for various compositions. We compare the critical separation for each composition with the cumulative fraction of captured planetesimal to estimate the fraction of ablated planetesimals. Tables and summarize these estimates for cluster and Field environments, respectively. In field environments, at most  $\sim 30\%$  of captured icy objects could be ablated, but only  $\sim 10\%$  rocky/iron bodies are ablated. In cluster environment, the number of icy objects lost to ablation is no more than  $\sim 12\%$ , for icy bodies, and which drops down to few per cent for rocky/iron compositions. For field environment there only two captured of 1 km planetesimals, therefore statistics are insignificant.

Field	$R_p = 1$ m	$R_p = 10$ m	$R_p = 10^2$ m	$R_p = 10^3$ m
Ice	< 0.01%	30%	28%	-
Carbonate	< 0.01%	21%	20%	-
Rock	< 0.01%	13%	13%	-
Iron	< 0.01%	8%	6%	-

Table 2: Fraction of captured planetesimals lost due to ablation in field environments.

## Disc structure and stopping conditions

We take the disc profile and drag coefficient prescription described in detail in ref. (16). We truncate the disc density at  $r_{\text{disc}} = 250$  AU. We initialize the planetesimal to start from  $r_0 = 20000$  AU with orbital parameters and disc inclination drawn from distributions described in the main text. We stop the simulation if the distance from the sun exceeds 50000 AU and negative energy and conclude the orbit is unbound. For bound orbits we stop if either the distance is  $r < 0.02$  AU or the orbital eccentricity is  $e < 0.1$ .

## References

1. K. J. Meech, *et al.*, *Nature* **552**, 378 (2017).
2. A. Do, M. A. Tucker, J. Tonry, *ArXiv e-prints* (2018).
3. F. C. Adams, D. N. Spergel, *Astrobiology* **5**, 497 (2005).
4. W. M. Napier, *MNRAS* **348**, 46 (2004).
5. P. S. Wesson, *SSR* **156**, 239 (2010).
6. M. Lingam, A. Loeb, *ArXiv e-prints* (2018).
7. H. F. Levison, M. J. Duncan, R. Brasser, D. E. Kaufmann, *Science* **329**, 187 (2010).
8. H. B. Perets, M. B. N. Kouwenhoven, *ApJ* **750**, 83 (2012).

9. M. Valtonen, *et al.*, *ApJ* **690**, 210 (2009).
10. E. Belbruno, A. Moro-Martín, R. Malhotra, D. Savransky, *Astrobiology* **12**, 754 (2012).
11. I. Adachi, C. Hayashi, K. Nakazawa, *Progress of Theoretical Physics* **56**, 1756 (1976).
12. S. J. Weidenschilling, *MNRAS* **180**, 57 (1977).
13. M. Čuk, J. A. Burns, *Icarus* **167**, 369 (2004).
14. E. Chiang, A. N. Youdin, *Annual Review of Earth and Planetary Sciences* **38**, 493 (2010).
15. C. W. Ormel, H. H. Klahr, *A&A* **520**, A43 (2010).
16. H. B. Perets, R. A. Murray-Clay, *ApJ* **733**, 56 (2011).
17. M. Lambrechts, A. Johansen, *A&A* **544**, A32 (2012).
18. T. Fujita, K. Ohtsuki, T. Tanigawa, R. Suetsugu, *AJ* **146**, 140 (2013).
19. E. Grishin, H. B. Perets, *ApJ* **811**, 54 (2015).
20. E. I. Chiang, P. Goldreich, *ApJ* **490**, 368 (1997).
21. P. Hut, J. Makino, S. McMillan, *ApJ Lett.* **443**, L93 (1995).
22. L. Dones, *et al.*, *Icarus* **142**, 509 (1999).
23. H. J. Melosh, *Astrobiology* **3**, 207 (2003).
24. J. B. Simon, P. J. Armitage, A. N. Youdin, R. Li, *ApJ Lett.* **847**, L12 (2017).
25. S. N. Raymond, P. J. Armitage, D. Veras, E. V. Quintana, T. Barclay, *ArXiv e-prints* (2017).
26. C. W. Ormel, H. Kobayashi, *ApJ* **747**, 115 (2012).

27. F. Windmark, *et al.*, *A&A* **540**, A73 (2012).
28. J. Blum, *ArXiv e-prints* (2018).
29. H. F. Levison, K. A. Kretke, M. J. Duncan, *Nature* **524**, 322 (2015).
30. R. A. Booth, F. Meru, M. H. Lee, C. J. Clarke, *MNRAS* **475**, 167 (2018).
31. A. Pinhas, N. Madhusudhan, C. Clarke, *MNRAS* **463**, 4516 (2016).
32. N. Ouellette, S. J. Desch, J. J. Hester, *ApJ* **711**, 597 (2010).
33. M. Bizzarro, *et al.*, *Science* **316**, 1178 (2007).
34. M. J. Burchell, J. R. Mann, A. W. Bunch, *MNRAS* **352**, 1273 (2004).

## Acknowledgments

We thank Barak A. Katzir and Andrei P. Igoshev for stimulating discussions. EG acknowledges support by the Technion Irwin and Joan Jacobs Excellence Fellowship for outstanding graduate students. EG and HBP acknowledge support by Israel Science Foundation I-CORE grant 1829/12 and the Minerva center for life under extreme planetary conditions.